Ammonia and nitrogen-based fertilizer production by solar-thermochemical processes

Cite as: AIP Conference Proceedings **2303**, 170016 (2020); https://doi.org/10.1063/5.0030980
Published Online: 11 December 2020

Josua Vieten, Dorottya Gubán, Martin Roeb, Bruno Lachmann, Sebastian Richter, and Christian Sattler

Ammonia and Nitrogen-based Fertilizer Production by Solar-thermochemical Processes

Josua Vieten,[1, 2 a)] Dorottya Gubán,[1, b)] Martin Roeb,[1, c)] Bruno Lachmann,[1] Sebastian Richter,[1, 2] and Christian Sattler [1, 2]

[1] *Institute of Solar Research, German Aerospace Center (DLR), Linder Hoehe, 51147 Cologne, Germany.*
[2] *Faculty of Mechanical Science and Engineering, Institute of Power Engineering, Professorship of Solar Fuel Production, 01069 Dresden, Germany.*

[a)] Corresponding author: Josua.Vieten@dlr.de
[b)] Dorottya.Guban@dlr.de
[c)] Martin.Roeb@dlr.de

Abstract. Ammonia is one of the most-produced chemicals in the world. It is applied in the fertilizer industry, and nitrogen fertilizers are a necessity to feed the world's growing population. Due to the high energy demand of the Haber-Bosch ammonia synthesis process, and due to the energy-intensive production of its precursors hydrogen and nitrogen, this process is associated with a significant carbon footprint. To reduce the greenhouse gas emissions of ammonia and fertilizer production, the authors develop solar-thermochemical routes for the production of nitrogen and hydrogen. Here we present an energetic optimization for combining pressure swing adsorption and thermochemical air separation to beat the energy efficiency of cryogenic air separation, and show recent results on materials development and experimental test campaigns of such two-step thermochemical redox cycles. We show that solar-thermochemical air separation is feasible and hint towards potential improvements of this technology and associated synergistic effects in fertilizer production. By this means, the CO_2 emissions of fertilizer production can be significantly reduced through application of concentrated solar energy. Future challenges include reactor design and heat recovery, as well as the selection of suitable redox materials.

INTRODUCTION

The demand for ammonia production has grown steadily over the last years and decades, already reached globally 200 million tons per year by 2018 and is forecasted to increase to over 350 million tons per year by 2050. [1] The application segment is dominated by the fertilizer industry, since the most important fertilizers are nitrogen-based and are produced from ammonia, which is synthesized via the Haber-Bosch process. The required hydrogen and nitrogen are currently provided by using fossil fuels. Hydrogen is mainly produced by natural gas reforming, whereas nitrogen is produced through cryogenic routes. This work proposes a two step novel approach consisting of the combination of pressure swing adsorption (PSA) and a thermochemical cycle for nitrogen production that potentially opens the way to produce ammonia from the raw materials water and air only by utilizing solar energy as reaction heat directly. The focus of the paper is on the nitrogen production part of the process, which requires air separation.

To separate air and generate a stream of nitrogen, several methods exist. The constituents of air can be separated physically by making use of their different boiling points (cryogenic air separation), their different adsorption rates, or based on molecular sieving. The latter two methods are the basis for pressure swing adsorption plants. Besides these physical separation methods, chemical methods exist as well, and materials such as titanium sponges have been used to strip oxygen off a gas stream for a long time. A more modern approach to this is thermochemical air separation, where a multivalent metal oxide is used as a reactant which reversibly binds oxygen. [2, 3] This process is especially appealing for application in concentrated solar plants, as thermal energy can be used directly without

SolarPACES 2019
AIP Conf. Proc. 2303, 170016-1–170016-10; https://doi.org/10.1063/5.0030980
Published by AIP Publishing. 978-0-7354-4037-1/$30.00

the inherent conversion losses of electricity generation. This process typically consists of two steps. One of them takes place at higher temperature and/or lower oxygen partial pressure, where the metal oxide is partially reduced (reduction step). The increased oxygen affinity of this partially reduced oxide is then used in a second step at lower temperature and/or higher oxygen partial pressure (oxidation step) to capture oxygen from a gas stream, allowing the metal ions to regain their initial oxidation state (Figure 1). The oxygen carrier material is in principle not consumed during this process. Such redox processes are often referred to as "chemical looping", and they can also be operated using other oxidants than air, such as water or CO_2. [4] In that case, water or CO_2 are split under the release of hydrogen or carbon monoxide, respectively. By that means, the hydrogen for ammonia production can be supplied using solar energy as well. However, the requirements for the redox material in terms of thermodynamic properties strongly differ between air separation and water/CO_2 splitting, as we will show later.

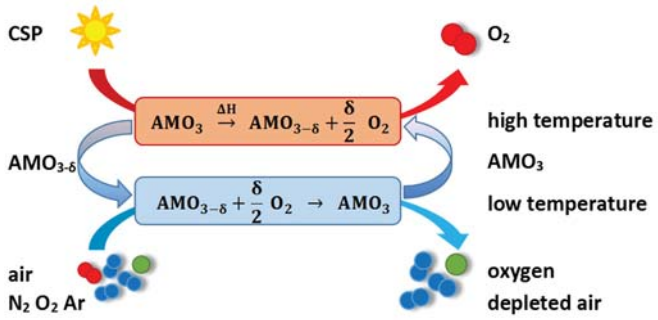

FIGURE 1. Chemical looping air separation process using a multivalent perovskite oxide $AMO_{3-\delta}$ with oxygen non-stoichiometry δ induced by reduction. The material is reduced at high temperature using concentrated solar power (CSP). Reproduced from [3] with permission from the Royal Society of Chemistry.

AIR SEPARATION MATERIALS

Thermochemical air separation can be performed with any material featuring temperature-dependent and fully reversible oxygen release and uptake. Materials investigated in the past include manganese, cobalt or copper oxides, since they feature multivalent metal ions. [2] Perovskites are another promising class of materials, since their composition can be tuned to match a wide range of different applications, and their properties can be adjusted by solid solution formation. [3, 5] Moreover, these materials react quickly, even at relatively low temperatures. [6] This allows performing many redox cycles per unit time and reduces the amount of material necessary for a fixed O_2/N_2 production rate.

Perovskite solid solutions have been studied both experimentally as well as using density functional theory (DFT) in a previous study. [7] For the DFT study, 2x2x2 superstructures of the cubic perovskite and the orthorhombic brownmillerite structure have been calculated, and atoms on the sites have been exchanged with occupancy fractions of 1/8 to simulate quinary oxides as solid solutions, such as $Sr_{0.875}Ba_{0.125}Fe_{0.875}Co_{0.125}O_{3-\delta}$. In this notation, $\delta = 0$ corresponds to the perovskite structure, while $\delta = 0.5$ is the brownmillerite. Redox enthalpies between the perovskite and the brownmillerite variant were calculated as the difference between the formation enthalpies obtained through DFT. Over 240 perovskites and their corresponding brownmillerites have been studied in this way, yielding a database of redox materials. Figure 2 shows the distribution of redox enthalpies in the entire dataset. In general, the redox enthalpy change upon reduction describes how readily the material releases oxygen under the formation of vacancies. Low redox enthalpy changes mean that the material is reduced readily and at lower temperatures. As a rule of thumb, materials which show redox enthalpy changes similar to the formation enthalpy of water may split water once reduced under the release of hydrogen, as described above, but of course, entropic effects play a role as well.

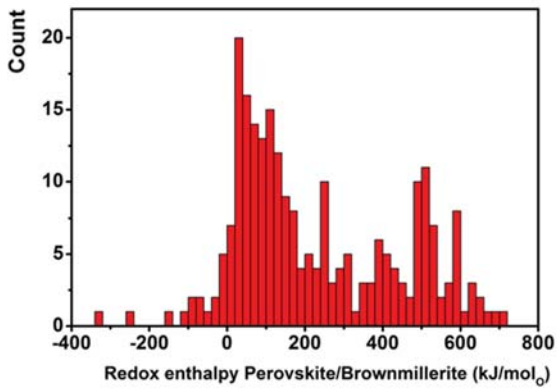

FIGURE 2. Distribution of redox enthalpies per mol of oxygen (O) between the perovskite and brownmillerite state from a theoretical study. [7] Negative redox enthalpies characterize inherently unstable materials. The higher the redox enthalpy, the more difficult (high temperature, low oxygen partial pressure) the reduction of the material, and the higher the oxygen affinity in the reduced state. Reprint from a thesis [8].

Air separation, however, does not require such high oxygen affinities of the reduced materials, and in order to limit the energy input of the entire process, materials should be chosen which are easier to reduce. $SrFeO_{3-\delta}$ is one of the materials often proposed for thermochemical air separation. [9, 10] Its redox enthalpy from perovskite to brownmillerite is 175.5 kJmol^{-1} O_2. [7, 11, 12] For instance, by creating a solid solution of $SrFeO_{3-\delta}$ with $SrMnO_{3-\delta}$, its redox enthalpy can be increased, which leads to a higher oxygen affinity in the reduced state, hence a lower oxygen partial pressure in the N_2 stream for air separation. [5] Figure 3 shows equilibrium oxygen partial pressures based on a thermodynamic model created from DFT data, [7] where ΔH and ΔS were calculated as functions of δ and T for a fixed value of $\delta = 0.20$. To account for the lower ionic radius of Mn^{4+} vs. Fe^{4+}, Sr^{2+} was partially substituted by Ca^{2+} in our calculations to maintain a stable perovskite crystal structure with a constant Goldschmidt tolerance factor of $t = 1.006$. [7] The data shows that the oxygen partial pressure in the produced nitrogen can easily reach values low enough for the Haber-Bosch production of ammonia, where the oxygen content should not exceed a few ppm. [13] It is important to point out that the oxygen partial pressure values shown in Figure 3 are for a fixed oxygen non-stoichiometry value in the respective perovskites.

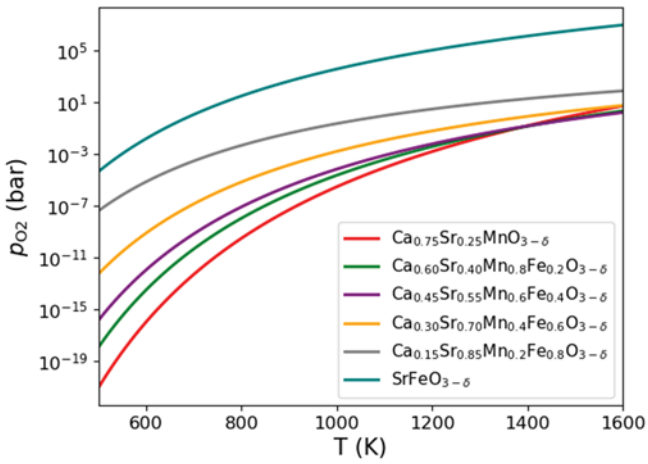

FIGURE 3. Calculated equilibrium oxygen partial pressure over different materials in the $(Ca,Sr)(Fe,Mn)O_{2.80}$ solid solution system at different temperature. The replacement of Fe by Mn leads to a higher redox enthalpy change and lower oxygen partial pressures in equilibrium. To maintain the same crystal structure, Sr^{2+} is partially replaced by Ca^{2+} which accounts for the lower ionic radius of Mn^{4+} vs. Fe^{4+}. Reprint from a thesis [8].

THE ENERGY DEMAND OF AIR SEPARATION

Fossil fuels are typically used as an energy source for ammonia production, which creates a large carbon footprint of 2.3 (metric) tons CO_2 per ton NH_3 when ammonia is produced using natural gas steam reforming. [14] While hydrogen production (0.5 t_{CO2}/t_{NH3}) and the Haber Bosch process itself (1,75 t_{CO2}/t_{NH3}) account for a significant portion of these emissions, the energy demand for cryogenic air separation (0,04 t_{CO2}/t_{NH3}) should not be neglected, especially since the nitrogen produced must be extremely pure, allowing only a few ppm of residual O_2 to avoid catalyst poisoning. [13] [15] This enables a reduction of CO_2 emissions through solar-thermochemical routes. Perovskite materials which can be used for thermochemical air separation such as $SrFeO_{3-\delta}$ are formed from earth-abundant, inexpensive materials. The drawback of such perovskites is their relatively low oxygen storage capacity of ≈ 2-4 wt%, which requires either a large amount of redox material or a high amount of redox cycles per time (which is possible due to the favorable oxidation and reduction kinetics of perovskites). This brings about a large sensible energy demand for the reduction step, as a lot of redox material has to be heated per mol of O_2 transferred. Moreover, the endothermic reduction process itself requires thermal energy.

In previous theoretical work by the authors based on density functional theory calculations, different perovskite redox materials have been identified with the respective lowest total thermal energy demand per mol of O_2 transferred under different conditions. [7, 8] All data can be retrieved from MPContribs, a user contribution interface of Materials Project (portal.mpcontribs.org). One example of these materials is $Sr_{0.875}Ba_{0.125}Fe_{0.875}Co_{0.125}O_{3-\delta}$. Under the assumption that this material is reduced at 1000 °C in an open reactor in air where oxygen is removed from the reaction zone solely by diffusion without additional pumping work, and re-oxidation is performed at 400 °C with an equilibrium target pressure of 10^{-6} bar (oxygen partial pressure), this material requires a thermal energy input of 2,217 $kJmol^{-1}$ O_2. Over 90% of this energy is stored as sensible heat in the material. An efficient thermochemical air separation process is therefore highly dependent on an efficient heat recovery system, as it helps lower the total energy demand by re-using heat released in the oxidation/cooling step for the next reduction/heating cycle. Another option to lower the total energy demand is to limit the temperature difference between reduction and oxidation by performing the reduction step at reduced oxygen partial pressure. If mechanical pumps are used for oxygen removal, a good estimate of the respective thermal energy input required for pumping is given by Brendelberger et al. [16] If we assume reduction at an oxygen partial pressure of 1 mbar, we can perform the reduction step at 600 °C and the oxidation step at 400 °C. The total energy demand per mol of O_2 using the same material is then lowered to 1,677 $kJmol^{-1}$ O_2 (59% sensible heat, 30% pumping, 11% endothermic reduction).

For comparison, cryogenic air separation requires a separation work of only 12 $kJmol^{-1}$ N_2. [17, 18] In the literature, this value is usually assumed to be independent of the N_2 purity, but in general, it should increase for very high purity levels, as multiple cryogenic air separation steps or additional purification may be necessary. For O_2 production, it has been shown that accepting lower product gas purity leads to a decrease in the energy demand of cryogenic air separation, but the effect is only in the order of about 10 %. [19] PSA systems, on the other hand, have a highly purity-dependent energy demand. With increasing product gas purity, the separation work increases. Typically, this behavior is approximated using the following relation, where w_{sep} is the separation work as a function of the oxygen partial pressure ratio of inlet and outlet: [17, 18]

$$w_{\mathrm{sep}} = \ln\left[\left(\frac{p_{\mathrm{O_2,in}}}{p_{\mathrm{O_2,out}}}\right)^2\right] \cdot 1000\ \mathrm{Jmol^{-1}} \tag{1}$$

From this equation, it follows that cryogenic air separation requires less work than PSA at N_2 purity levels of under 500 ppm residual oxygen. This is the reason why most Haber Bosch plants currently still rely on cryogenic air separation – PSA systems cannot achieve the required oxygen purity under comparable energy demand. Exceptions may hold for small scale plants, as the energy demand for cryogenic air separation increases significantly at smaller plant sizes. [19]

Thermochemical air separation comes with the advantage of using thermal energy from concentrated sunlight directly instead of electricity. Therefore, we need to convert the electrical work of state-of-the-art technologies as given by Eq. 1 or Ref. [17, 18] to a thermal energy input for comparison. Assuming a thermal power plant efficiency of 30 % (heat to net electricity output), the thermal energy demand of cryogenic air separation reaches 40 $kJmol^{-1}$ N_2. However, this is still orders of magnitude below the value for thermochemical air separation. It becomes obvious that thermochemical air separation on its own as sole technology for air separation cannot compete with state of the art technologies in most cases, with the exception of small scale high purity systems. However, the

energy demand of thermochemical air separation processes can be decreased drastically by recovering the heat released during the oxidation step and re-using it for the next reduction step. In the case of our exemplary perovskite oxide, an overall heat recovery rate of 97% would be required to reach total energy demands comparable with cryogenic systems. [8] Considering that this heat would have to be recovered between solids which must not be in direct contact with each other to avoid oxygen transfer, it appears extremely challenging to achieve such values. Previous work has shown maximum solid-solid heat recovery rates of 30-80 % for such systems. [20]

Nevertheless, combining thermochemical air separation with PSA allows the overall process to be operated at lower thermal energy demand than cryogenic air separation while reaching high product purities. The energy required to transfer one mol of O_2 is virtually independent of its concentration in thermochemical pumps. [16] This holds true as long as the redox material is operated in a range not too close to its fully reduced or fully oxidized state, which is the case for our exemplary material in the selected temperature and pressure range. This renders this process very appealing for achieving very high purity N_2 (and O_2) streams. If the bulk of the oxygen is removed by a PSA system to pre-purify the air, and the remaining oxygen is then removed by thermochemical means, only a small molar amount of O_2 molecules have to be transferred thermochemically to achieve a significant output of high-purity N_2. The high energy demand of thermochemical air separation therefore becomes less significant in the total thermal energy balance, instead the thermochemical pump serves as a secondary purifier, combined with a cheap and energy efficient PSA system with relatively low output purity for ammonia production. In the energy balance, q_{sep} is the total thermal energy required for air separation in the combined system, η_{elec} is the efficiency of electricity generation in the CSP plant ($\eta_{\mathrm{elec}} = 0.3$ in this work), Ψ is the heat recovery rate of the thermochemical air separator, $q_{\mathrm{thermochem}}$ is the energy demand of thermochemical air separation per mol of O_2, and $p_{\mathrm{O_2,trans}}$ is the residual oxygen content at the PSA outlet we call "transition purity", i.e., the oxygen partial pressure in the N_2 stream at the PSA outlet:

$$q_{\mathrm{sep}} = \ln\left[\left(\frac{p_{\mathrm{O_2,in}}}{p_{\mathrm{O_2,trans}}}\right)^2\right] \cdot \eta_{\mathrm{elec}}^{-1} \cdot 1000\ \mathrm{J mol^{-1}} + q_{\mathrm{thermochem}} \cdot p_{\mathrm{O_2,trans}} \cdot \psi \cdot \mathrm{mol\ bar^{-1}} \quad (2)$$

For a given redox material, q_{sep} becomes virtually independent of the target nitrogen purity below the transition purity. Nevertheless, $q_{\mathrm{thermochem}}$ is a material dependent property, and depends on the target purity. q_{sep} is therefore indirectly dependent on the product gas purity, but in our case the effect of the target purity on the total energy demand is negligible. Values for different materials under different conditions can be generated in our online tool *RedoxThermoCSP* as a user contribution to *Materials Project* (portal.mpcontribs.org).

From Eq. 2, it can be shown that a combined solar PSA and thermochemical system can be operated more efficiently than a solar-electrical cryogenic system. The calculation assumes that oxygen is removed from air using a PSA system until the "transition purity" is reached. The pre-purified nitrogen then leaves the PSA with a significant amount of residual oxygen, which is subsequently removed thermochemically. An exemplary calculation highlighting the advantage of combining a PSA and a thermochemical pump is shown in Figure 4. Graph (a) shows a calculation for $Sr_{0.875}Ba_{0.125}Fe_{0.875}Co_{0.125}O_{3-\delta}$ as a redox material for air separation, which is oxidized at 400 °C and reduced at 600 °C using a vacuum pump to maintain 10^{-3} bar oxygen partial pressure during reduction. [7, 8] at a fixed target N_2 purity of 1 ppm residual oxygen ($p_{O_2} = 10^{-6}$ bar) with the respective thermal energy demand of a solar-thermal PSA and cryogenic air separator (AS) at $\eta_{elec} = 0.3$. The electrical energy is assumed to be generated from thermal energy. The grey curves show the total energy demand of a combined PSA and thermochemical pump at different transition purities, i.e. different partial pressures of residual oxygen at the PSA outlet. The higher the solid-solid heat recovery rate in the thermochemical system, the wider becomes the range in which it is more efficient than the PSA system, and the higher the ideal transition purity becomes where the total energy demand is minimized. Additionally, the minimum total energy demand decreases. At realistic heat recovery rates (30-60 %), the total energy demand can be 24-45 % lower than with a cryogenic system powered through electricity generated from solar-thermal heat. The energy efficiency could be even higher if materials and operating conditions are further optimized.

Graph (b) in Figure 4 shows an exemplary process where the system is operated with 60 % heat recovery efficiency and at the optimum transition purity from graph (a) of 10^{-2} bar (i.e., a PSA with 99% N_2 purity if O_2 is the only impurity). The total energy demand is shown as a function of the final purity of the produced N_2. The dashed vertical line indicates the transition purity. As discussed before, assuming a constant energy demand of cryogenic air separation and the combined PSA and thermochemical pump is reasonable under the conditions applied. The strength of a combined PSA and thermochemical system is that it combines the low energy demand of a PSA system

with the virtual independence of the separation energy input on the target purity of a thermochemical system within the constraints of the material applied.

As a redox material for thermochemical air separation the perovskite $Sr_{0.875}Ba_{0.125}Fe_{0.875}Co_{0.125}O_{3-\delta}$ is used, which is oxidized at 400 °C and reduced at 600 °C using a vacuum pump to maintain 10^{-3} bar oxygen partial pressure during reduction. [7, 8]

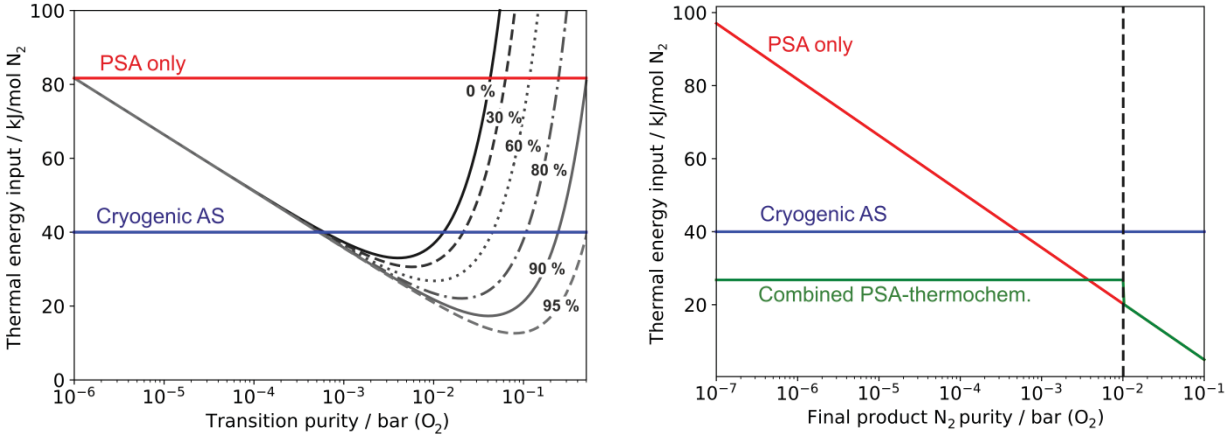

FIGURE 4. Calculated thermal energy input (solar-thermal heat) for air separation under different conditions. (a) Energy input assuming a target nitrogen purity of 10^{-6} bar residual oxygen partial pressure. Grey lines indicate the energy demand of a combined PSA and thermochemical pump at different solid-solid heat recovery efficiencies in dependence of the transition purity, i.e., the residual concentration of O_2 after the PSA stage. These values are compared to cryogenic air separation (AS) and PSA only. (b) Energy demand for air separation with different final N_2 target purities at a solid-solid heat recovery efficiency of 60 %. The dashed vertical line indicates the transition purity, which is the minimum of the 60%-curve in the left graph.

Our data shows that nitrogen at a purity level meeting the standards for Haber-Bosch plants can be obtained energetically more efficiently than through PSA by combining a PSA system and a thermochemical system. This holds true that the PSA gas outlet does not contain significant amounts of gases other than N_2 or O_2, or that these impurities can be removed at low additional cost. Efficient solid-solid heat recovery routes help increase the system efficiency, but it is remarkable that even if no heat is recovered, a combined PSA and thermochemical system uses the thermal energy of a concentrating solar plant more efficiently than an cryogenic air separator operated with electrical energy generated through CSP. Our calculation neither accounts for thermal losses, nor for potential further improvements of the redox material and operating conditions. Moreover, the effect of scale is not accounted for – in small scale ammonia plants, a combination of thermochemical and PSA air separation systems is expected to be even more valuable, as cryogenic air separation plants typically require large scale plants to be efficient.

It is worth noting that even if electrical energy is used instead of thermal energy for PSA, cryogenic AS, or the thermochemical setup, the electrical energy demand w_{sep} of a combined PSA and thermochemical system is lower than for cryogenic AS if the solid-solid heat recovery rate in the thermochemical system is higher than 15% in an exemplary calculation for $Sr_{0.875}Ba_{0.125}Fe_{0.875}Co_{0.125}O_{3-\delta}$ according to

$$w_{\mathrm{sep}} = \ln\left[\left(\frac{p_{\mathrm{O_2,in}}}{p_{\mathrm{O_2,trans}}}\right)^2\right] \cdot 1000\ \mathrm{J mol^{-1}} + q_{\mathrm{thermochem}} \cdot p_{\mathrm{O_2,trans}} \cdot \psi \cdot \mathrm{mol\ bar^{-1}} \quad (3)$$

In that case, the optimized transition purity is about one order of magnitude lower than in the example shown in Figure 4, since the PSA system is significantly more efficient if electrical energy is used directly instead of when converting thermal to electrical energy at η_{elec}.

PROOF OF CONCEPT

Thermochemical air separation using perovskites as redox materials was demonstrated by laboratory scale experiments. The initial calculations showed that $SrFeO_{3-\delta}$ is a promising candidate, as well as cheap, non-toxic material that can be easily synthesized by well-known ceramic routes. The above-mentioned material $Sr_{0.875}Ba_{0.125}Fe_{0.875}Co_{0.125}O_{3-\delta}$ is an optimized variant of $SrFeO_{3-\delta}$ which will be tested in future experiments. $SrCO_3$ and Fe_3O_4 were mixed in stoichiometric ratio, and then annealed at 1100 ºC for 20 hours in air. The sintered block was ball milled and spherical particles with a diameter of 2 mm were formed via a modified mixing-spheronization method. 50 g of the produced particles were filled in an IR-heated tube furnace. Five redox cycles were performed, while the in- and outlet oxygen concentrations were monitored. The reduction step was performed at 800 °C in Ar flow, whereas the oxidation took place at 350 °C in synthetic air. In order to investigate the effect of coupling the thermochemical cycle with a PSA unit, the experiments were repeated with oxidation in N_2 flow that contains a reduced amount of O_2 of 1%. [9]

The results showed that during the air purification step oxygen partial pressures of approximately 3 × 10−6 bar were reached in both set of experiments as shown in Fig. x. When removing oxygen from air, the 50 grams of material produced in total 0.602-0.662 l of gas with less than 10 ppm of oxygen impurities. When removing oxygen from a semi-purified stream, the same amount of material produced 2.014-2.661 l of gas with the same purity. The good agreement between the curves of different cycles shows the excellent repeatability of the process and lack of degradation of the material, at least over the limited number of cycles performed.

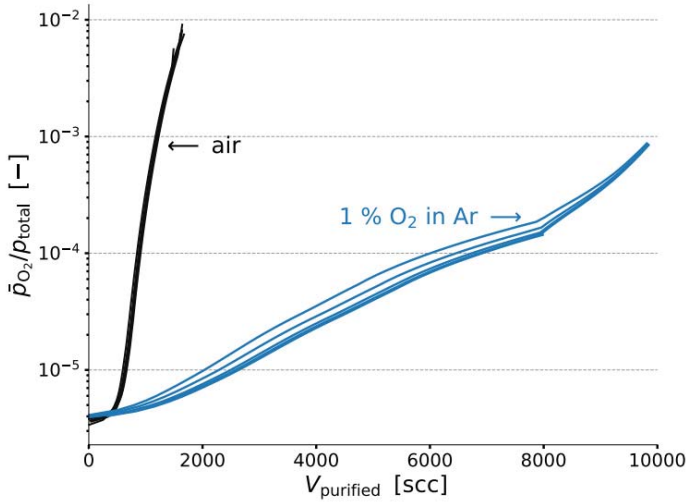

FIGURE 5. Residual oxygen content in a stream of gas separated from air and a test gas using $SrFeO_{3-\delta}$ in an infrared furnace test setup. Using a test gas with 1 % O_2 in Ar simulating the PSA output, a significantly higher amount of gas with oxygen content in the range of a few ppm is produced with the same amount of redox material, showcasing the higher efficiency in this case. Reproduced with permission from Elsevier. [9]

EXPERIMENTAL VALIDATION OF SOLAR REDUCTION OF THE REDOX PARTICLES

The laboratory scale experiments showed that nitrogen with the required purity can be produced by the suggested thermochemical cycle. The regeneration of the oxygen sorption capacity of the redox particles requires to reduce them at elevated temperatures and/or lower oxygen partial pressures. The required higher temperature can be provided in a sustainable way via concentrated solar energy. A directly irradiated solar rotary kiln was designed to demonstrate the reduction step. In order to monitor the oxygen release of the particles an oxygen sensor was attached to the outlet gas pipeline, and a gas-tight design was realized by using a quartz window. The experimental setup is shown on Fig. 6.

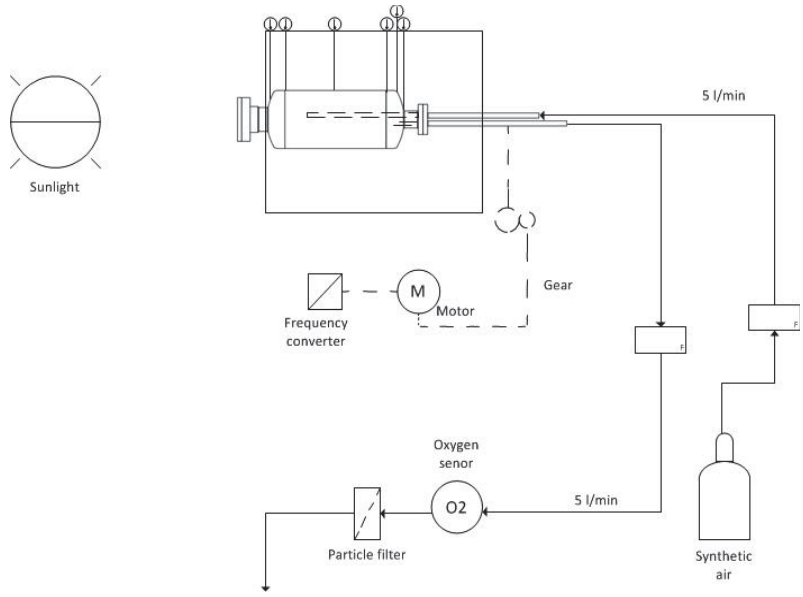

FIGURE 6 Experimental setup for solar reduction of the $SrFeO_x$ redox material

The reactor was filled with 250 g $SrFeO_x$ particles with a diameter of 2 mm and heated by concentrated sunlight in the solar furnace of DLR, Cologne under a constant air flow to the reduction temperature, while the outlet oxygen concentration was continuously monitored. The temperature and oxygen concentration patterns are shown on Fig 7 a and b. An even heating rate was achieved, while a temperature gradient was observed in the length of the reactor with a difference of 100-300 °C, but 600 °C was reached throughout the entire reactor, which appeared to be the minimum required temperature for reduction. Upon reaching a temperature of 600 °C a clear increase in the oxygen concentration was observed, which indicates onset of the reduction reaction. The temperature was held until the peak in the oxygen concentration relaxed, then the reactor was cooled and re-oxidization of the particles occurred. The analysis of the reduction and oxidation showed that during the reduction 4 l oxygen was released, and 3.6 l was recaptured, which indicates a nearly complete reduction and 90% of the reduced particles were re-oxidized.

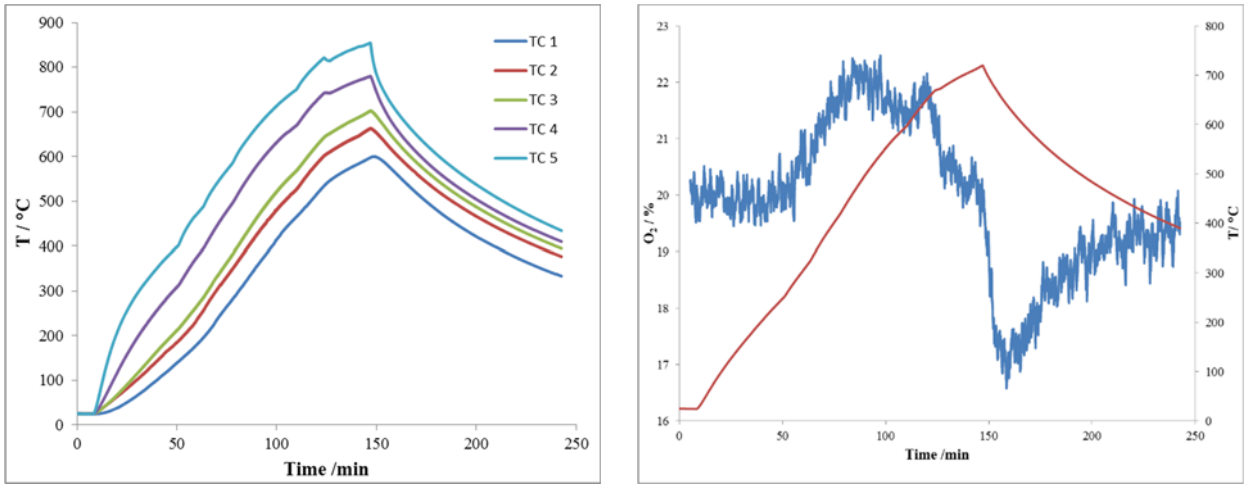

(a) (b)

FIGURE 7. Solar reduction of SrFeOx redox particles under air flow. a) Temperature distribution throughout the length of the reactor (TC1-5 front towards the back). b) Blue line: Oxygen concentraction in the outlet gas flow, Red line: average reactor temperature.

OUTLOOK AND SYNERGISTIC EFFECTS

The laboratory scale demonstration of the concept proved that nitrogen with O_2 impurity levels suitable for the Haber Bosch process can be produced by using thermochemical cycles; furthermore it showed the potential in using a pre-purified gas mixture provided by the PSA unit. Using a combined PSA and thermochemical setup is energetically very efficient, and allows to use a larger fraction of the energy directly as heat, which is beneficial in a concentrated solar thermal system. The experiments in the solar rotary kiln demonstrated the solar reduction of the redox particles, which occurred also under air atmosphere.

The next step is to experimentally validate a combined PSA and thermochemical system, and then investigate the whole fertilizer production process to find the possible synergistic effects with the introduced air separation method. In the reduction step of the thermochemical cycle oxygen is released. The produced oxygen-enriched air during the reduction step can also be captured and utilized in the fertilizer production process. One of the most commonly used N-fertilizers is ammonium-nitrate, which is synthesized from nitric acid and ammonia precursors. The state-of-art method for HNO_3 production is the Ostwald process, a two-step oxidation reaction of ammonia. In the first, highly exothermic step NH_3 is oxidized to NO with a PtRh catalyst, while in the second reaction step NO is further oxidized to NO_2 in air. Studies showed that an increased O_2 concentration in the second step can increase the nitric acid production capacity; [21, 22] therefore the use of the produced O_2-enriched air from the air separation unit would provide a further benefit.

In summary, we demonstrated how thermochemical air separation can ideally complement a pressure swing adsorption process, yielding nitrogen at purity rates sufficient for Haber-Bosch ammonia production. Selecting suitable perovskite materials based on theoretical considerations allows an optimization towards the desired process conditions. Further work will focus on a scale-up to pre-industrial scale, and an investigation of synergistic effects when using the oxygen separated from air for nitric acid production, including the entire value chain for fertilizer production using solar energy.

ACKNOWLEDGMENTS

This work has received funding within the project DÜSOL (EFRE-0800603) which is co-funded in the "Klimaschutzwettbewer ErneuerbareEnergien.NRW" by the state of Northrhine-Westphalia, Germany, and the European EFRE fund.

REFERENCES

1. *U.S. Geological Survey, Mineral Commodity Summaries*. 2015.
2. Moghtaderi, B., *Application of Chemical Looping Concept for Air Separation at High Temperatures.* Energy & Fuels, 2010. **24**(1): p. 190-198.
3. Vieten, J., et al., *Perovskite oxides for application in thermochemical air separation and oxygen storage.* Journal of Materials Chemistry A, 2016. **4**(35): p. 13652-13659.
4. Agrafiotis, C., M. Roeb, and C. Sattler, *A review on solar thermal syngas production via redox pair-based water/carbon dioxide splitting thermochemical cycles.* Renewable and Sustainable Energy Reviews, 2015. **42**: p. 254-285.
5. Vieten, J., et al., *Redox thermodynamics and phase composition in the system SrFeO3 − δ — SrMnO3 − δ.* Solid State Ionics, 2017. **308**: p. 149-155.
6. Vieten, J., et al., *Redox Behavior of Solid Solutions in the SrFe1-xCuxO3-δ System for Application in Thermochemical Oxygen Storage and Air Separation.* Energy Technology, 2019. **7**(1): p. 131-139.
7. Vieten, J., et al., *Materials design of perovskite solid solutions for thermochemical applications.* Energy & Environmental Science, 2019. **12**(4): p. 1369-1384.
8. Vieten, J., *Perovskite Materials Design for Two-Step Solar-Thermochemical Redox Cycles*. 2019, TU Dresden.
9. Bulfin, B., et al., *Air separation and selective oxygen pumping via temperature and pressure swing oxygen adsorption using a redox cycle of SrFeO3 perovskite.* Chemical Engineering Science, 2019. **203**: p. 68-75.
10. Loutzenhiser, P.G., et al., *CO2 Splitting via Two-Step Solar Thermochemical Cycles with Zn/ZnO and FeO/Fe3O4 Redox Reactions II: Kinetic Analysis.* Energy & Fuels, 2009. **23**(5): p. 2832-2839.

11. Jain, A., et al., *The Materials Project: Accelerating Materials Design Through Theory-Driven Data and Tools*, in *Handbook of Materials Modeling : Methods: Theory and Modeling*, W. Andreoni and S. Yip, Editors. 2018, Springer International Publishing: Cham. p. 1-34.
12. Jain, A., et al., *Formation enthalpies by mixing GGA and GGA $+$ U calculations.* Physical Review B, 2011. **84**(4): p. 045115.
13. Jennings, J.R., *Catalytic Ammonia Synthesis: Fundamentals and Practice*. 2013: Springer US.
14. Rafiqul, I., et al., *Energy efficiency improvements in ammonia production—perspectives and uncertainties.* Energy, 2005. **30**(13): p. 2487-2504.
15. A. K. Hill, C.S.L.T.-M., *Current and future role of Haber-Bosch ammonia in a carbon-free energy landscape.* Energy Environ. Sci, 2020. **13**: p. 331-344.
16. Brendelberger, S., et al., *Vacuum pumping options for application in solar thermochemical redox cycles – Assessment of mechanical-, jet- and thermochemical pumping systems.* Solar Energy, 2017. **141**: p. 91-102.
17. Krenzke, P.T. and J.H. Davidson, *On the Efficiency of Solar H2 and CO Production via the Thermochemical Cerium Oxide Redox Cycle: The Option of Inert-Swept Reduction.* Energy & Fuels, 2015. **29**(2): p. 1045-1054.
18. Li, S., et al., *Thermodynamic Analyses of Fuel Production via Solar-Driven Non-stoichiometric Metal Oxide Redox Cycling. Part 2. Impact of Solid–Gas Flow Configurations and Active Material Composition on System-Level Efficiency.* Energy & Fuels, 2018. **32**(10): p. 10848-10863.
19. Banaszkiewicz, T., M. Chorowski, and W. Gizicki, *Comparative analysis of cryogenic and PTSA technologies for systems of oxygen production.* AIP Conference Proceedings, 2014. **1573**(1): p. 1373-1378.
20. Felinks, J., et al., *Heat recovery concept for thermochemical processes using a solid heat transfer medium.* Applied Thermal Engineering, 2014. **73**(1): p. 1006-1013.
21. Hui, S., et al., *Effect of oxygen on N2O and NO formation from NH3 oxidation over MnOx/TiO2 catalysts.* Energy Procedia, 2019. **158**: p. 1497-1501.
22. Bahtia, S., et al., *Patent EP0799794A1, Oxygen injection in nitric acid production*. 1997.